



This is a repository copy of *Tensor electrical impedance myography identifies bulbar disease progression in amyotrophic lateral sclerosis.*

White Rose Research Online URL for this paper:
<https://eprints.whiterose.ac.uk/186797/>

Version: Published Version

Article:

Schooling, C.N., Healey, T.J., McDonough, H.E. et al. (5 more authors) (2022) Tensor electrical impedance myography identifies bulbar disease progression in amyotrophic lateral sclerosis. *Clinical Neurophysiology*, 139. pp. 69-75. ISSN 1388-2457

<https://doi.org/10.1016/j.clinph.2022.04.015>

Reuse

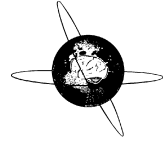
This article is distributed under the terms of the Creative Commons Attribution (CC BY) licence. This licence allows you to distribute, remix, tweak, and build upon the work, even commercially, as long as you credit the authors for the original work. More information and the full terms of the licence here:
<https://creativecommons.org/licenses/>

Takedown

If you consider content in White Rose Research Online to be in breach of UK law, please notify us by emailing eprints@whiterose.ac.uk including the URL of the record and the reason for the withdrawal request.



eprints@whiterose.ac.uk
<https://eprints.whiterose.ac.uk/>



Tensor electrical impedance myography identifies bulbar disease progression in amyotrophic lateral sclerosis



Chlöe N. Schooling^{a,b,*}, T.Jamie Healey^c, Harry E. McDonough^a, Sophie J. French^a, Christopher J. McDermott^a, Pamela J. Shaw^a, Visakan Kadirkamanathan^b, James J.P. Alix^{a,*}

^aSheffield Institute for Translational Neuroscience, University of Sheffield, UK

^bDepartment of Automatic Control and Systems Engineering, University of Sheffield, UK

^cDepartment of Clinical Engineering, Sheffield Teaching Hospitals NHS Foundation Trust, UK

ARTICLE INFO

Article history:

Accepted 15 April 2022

Available online 5 May 2022

Keywords:

Amyotrophic lateral sclerosis

Biomarker

Electrical impedance myography

Tongue

Bulbar

Disease progression

HIGHLIGHTS

- Tensor electrical impedance myography reduces complex multi-frequency, multi-electrode configuration impedance data down to a single metric.
- This metric captures disease progression more sensitively than other bulbar disease biomarkers, including tongue strength and the ALS-FRS-R.
- Tensor electrical impedance myography improves the bulbar biomarker potential of electrical impedance measurements in ALS.

ABSTRACT

Objective: Electrical impedance myography (EIM) is a promising biomarker for amyotrophic lateral sclerosis (ALS). A key issue is how best to utilise the complex high dimensional, multi-frequency data output by EIM to fully characterise the progression of disease.

Methods: Muscle volume conduction properties were obtained from EIM recordings of the tongue across three electrode configurations and 14 input frequencies (76 Hz–625 kHz). Analyses of individual frequencies, averaged EIM spectra and non-negative tensor factorisation were undertaken. Longitudinal data were collected from 28 patients and 17 healthy volunteers at 3-monthly intervals for a maximum of 9 months. EIM was evaluated against the Amyotrophic Lateral Sclerosis Functional Rating Scale-Revised (ALSFRS-R) bulbar sub-score, tongue strength and an overall bulbar disease burden score.

Results: Longitudinal changes to individual patient EIM spectra demonstrated complex shifts in the spectral shape. At a group level, a clear pattern emerged over time, characterised by an increase in centre frequency and general shift to the right of the spectral shape. Tensor factorisation reduced the spectral data from a total of 168 data points per participant per recording to a single value which captured the complexity of the longitudinal data and which we call tensor EIM (T-EIM). The absolute change in tensor EIM significantly increased within 3 months and continued to do so over the 9-month study duration. In a hypothetical clinical trial scenario tensor EIM required fewer participants ($n = 64$ at 50% treatment effect), than single frequency measures (n range 87–802) or ALSFRS-R bulbar subscore ($n = 298$).

Conclusions: Changes to tongue EIM spectra over time in ALS are complex. Tensor EIM captured and quantified disease progression and was more sensitive to changes than single frequency EIM measures and other biomarkers of bulbar disease.

Significance: Objective biomarkers for the assessment of bulbar disease in ALS are lacking. Tensor EIM enhances the biomarker potential of EIM data and can improve bulbar symptom monitoring in clinical trials.

Crown Copyright © 2022 Published by Elsevier B.V. on behalf of International Federation of Clinical Neurophysiology. This is an open access article under the CC BY license (<http://creativecommons.org/licenses/by/4.0/>).

Abbreviations: ALS, Amyotrophic Lateral Sclerosis; ALS-FRS-R, ALS Functional Rating Scale-Revised; EIM, Electrical Impedance Myography; EMG, Electromyography; NTF, Non-negative Tensor Factorisation; PCA, Principal Component Analysis; Δ T-EIM, Change in Tensor EIM.

* Corresponding authors at: Sheffield Institute for Translational Neuroscience, University of Sheffield, 385A Glossop Road, S10 2HQ, UK.

E-mail addresses: cnschooling1@sheffield.ac.uk (C.N. Schooling), j.alix@sheffield.ac.uk (J.J.P. Alix).

<https://doi.org/10.1016/j.clinph.2022.04.015>

1388–2457/Crown Copyright © 2022 Published by Elsevier B.V. on behalf of International Federation of Clinical Neurophysiology.

This is an open access article under the CC BY license (<http://creativecommons.org/licenses/by/4.0/>).

1. Introduction

Electrical impedance myography (EIM) is a simple to use candidate biomarker for neuromuscular diseases. The pioneering work of Rutkove and colleagues has demonstrated its effectiveness across a range of disorders, including amyotrophic lateral sclerosis (ALS) (Rutkove and Sanchez, 2019; Mcilduff et al., 2017). Data are generated by the application alternating current (AC) and measurement of the resulting surface voltage (Rutkove and Sanchez, 2019). The frequency dependent effects of cell membrane capacitance and the resistive effects of the intra-/extracellular compartments mean that tissue is more fully characterised via a range of AC frequencies, an impedance spectrum (Holder, 2004).

A key question within EIM is how best to utilise the full spectrum of data. Most work has utilised a limited number of frequency outputs, even when a wide frequency spectrum has been collected (e.g., (Mcilduff et al., 2017)). More complete use of the frequency range has been attempted, either using reactance only measurements (Kapur et al., 2019), or a selection of different frequencies (Alix et al., 2020). In order to make use of the complete frequency spectrum we have recently developed an analysis technique which we term “tensor EIM”. The aim of the tensor EIM is to aggregate and simplify the large amount of EIM data, while minimising any loss of information. This is done using a mathematical procedure known as non-negative tensor factorisation, which has been applied to several areas of medicine (Escudero et al., 2015; Aram et al., 2015; Xie and Song, 2013). In EIM, where there can be both multiple input frequencies and multiple electrode arrangements, tensor EIM has the advantage of analysing all the information gained across all of these frequencies/configurations. Dominant patterns in the data are then identified and their importance quantified as a single ‘score’, which in previous work was able to correctly classify patients with ALS and correlated with disease severity (Schooling et al., 2021).

In ALS, quantitative measures of disease change over time are of increasing importance as several promising therapeutics reach clinical trials (Calabrese et al., 2021; Bald et al., 2021). While longitudinal EIM studies in ALS have used only a small amount of the available data, power analyses indicate that significant improvements in trial design can be achieved through limb EIM measurements (Rutkove et al., 2012; Shefner et al., 2018). Bulbar disease monitoring in trials is often limited (Yunusova et al., 2019) and the most commonly assessed muscle, the tongue, provides additional challenges relating to the complexity of the myo-architecture (Gage et al., 2017). With fibres running in multiple orientations, multiple frequencies and electrode configurations may be required to sensitively detect disease, resulting in a large and complicated EIM dataset.

Adding to this complexity are the contrasting effects muscle changes in ALS would be expected to have an impedance spectrum, as denervation is followed by reinnervation, which is then punctuated with further episodes of denervation and ultimately reinnervation failure. In preclinical studies utilising sciatic nerve ligation, changes to impedance spectra in the acute setting were both short lived and different to those observed in a chronic setting (Carlson, 2014; Ahad et al., 2010). Later work with the SOD1^{G93A} mouse model demonstrated resistance decreased in the pre-symptomatic stage and then increased in the symptomatic stage (Li et al., 2016).

On the basis of such observations, we hypothesised that in ALS the longitudinal changes in EIM spectra from individual patients would be complex, owing to the competing effects of acute and chronic denervation/reinnervation. To investigate this, we employed multi-directional tongue EIM recordings and captured the dominant spectral patterns with tensor EIM. By utilising data

from a range of frequencies (i.e. the impedance spectrum) we demonstrate a more sensitive detection of disease-related impedance changes.

2. Methods

2.1. Data collection

Patients meeting any of the three levels of the Awaji-Shima criteria for ALS were recruited through the specialist motor neurone disease clinic at the Royal Hallamshire Hospital, Sheffield, UK. (De Carvalho et al., 2008). Longitudinal EIM tongue measurements were made in 28 ALS patients (11, male, 17 female), with a mean age of 60 years (range 30–77). At baseline visit patients had a mean disease duration of 49 months (range: 5–204) and mean bulbar symptom duration of 30 months (range: 0–204). Measurements were made at baseline, 3, 6 and 9 months, with some attrition in patient numbers seen over time (Table 1). Additionally, 20 healthy control subjects (9 male, 11 female; mean age 51 years, range 22–82) were studied at baseline and 6 months.

EIM recordings were recorded utilising three 3-dimensional electrode configurations in which current and voltage sense electrodes were on opposite surfaces of the tongue (Fig. 1a). Measurements were made on both the central and lateral portions of the tongue blade (Fig. 1b), which have previously shown to be sensitive and specific for disease detection (Schooling et al., 2020). The spectra were recorded at 14 frequency values starting at 76 Hz and doubling each step up to 625 kHz. The impedance values were calibrated to give volume conducted potential (VCP) values, as proposed by (Sanchez et al., 2021). For these the cell constant of each electrode configuration was used to calibrate the impedance. The volume independent impedivity values obtained provide a standardised measure of the passive electrical properties of tissue, with the advantage that data from different electrode configurations can be directly compared and combined (Luo et al., 2021; Sanchez et al., 2021).

In addition to EIM data, the amyotrophic lateral sclerosis functional rating scale-revised (ALSF_{RS}-R) bulbar sub-score was completed at each visit and a thorough clinical bulbar examination performed. Clinical signs of disease (wasting, weakness and fasciculations) were quantified by a simple scoring system (Table 2). Tongue strength recordings were also undertaken using the Quantitative Muscle Testing system (Averil Medical), coupled to the Iowa Oral Performance Instrument (Shellikeri et al., 2015). A comprehensive bulbar disease burden score was calculated by combining the ALSFR_S-R, tongue strength and clinical examination signs into a score out of 36, with a lower value representing more severe disease (Schooling et al., 2021). The rate of symptom change was calculated for each patient as the change in bulbar disease burden score divided by the number of months for which the change was measured.

Details on the collection of Electromyography (EMG) data are outlined in Supplementary Methods S1.

2.2. Tensor EIM method

Each participant at each visit generated 168 data values (see Fig. 1c). These complex data were simplified in two steps. First,

Table 1
Number of participants (patients and healthy) recorded on at each time point.

Visit	Patients	Healthy
Baseline	28	20
3 Months	26	
6 Months	20	20
9 Months	14	

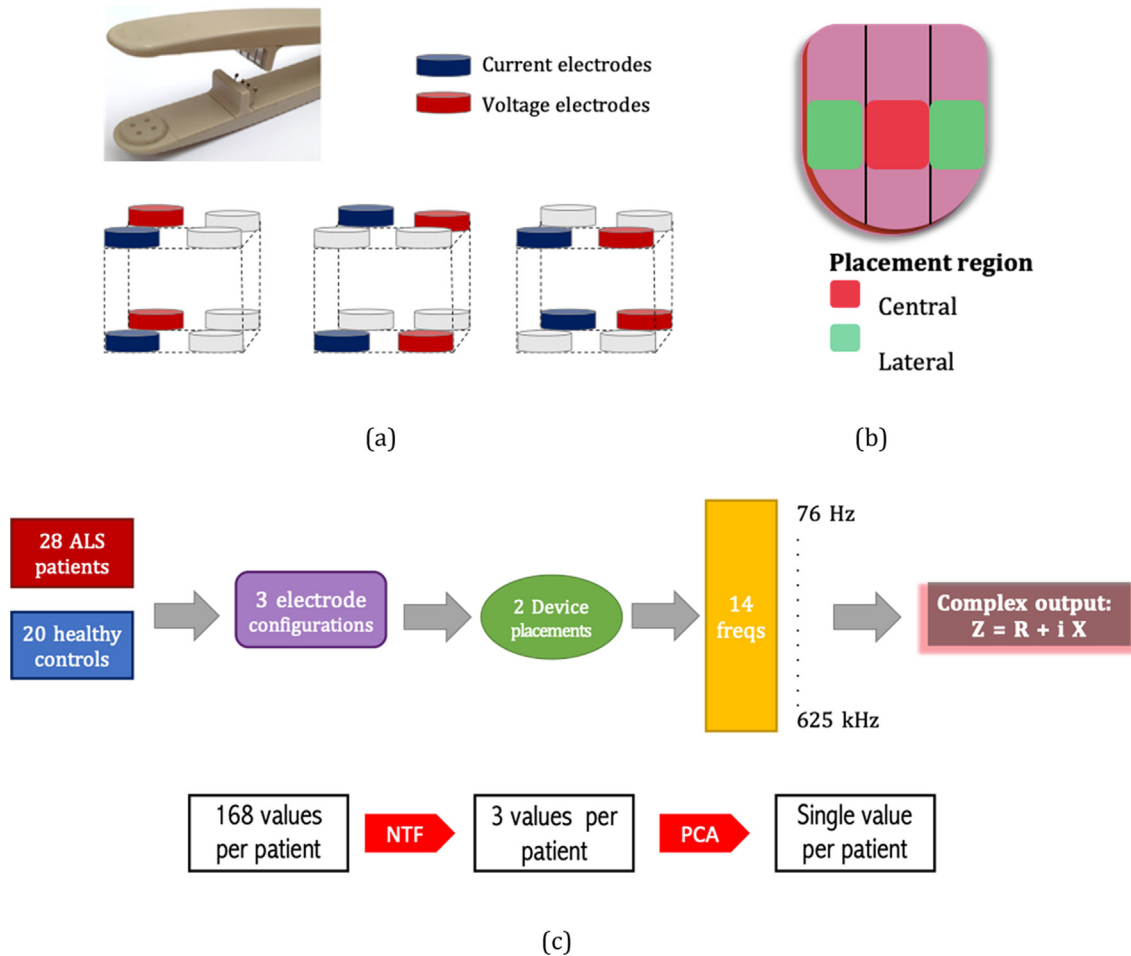


Fig. 1. (a) The tongue EIM (electrical impedance myography) device holds tissue between the two recording plates of the probe and records over a fixed tissue volume. Electrode arrangements used are shown in the schematic. (b) The placement areas for central and lateral recordings. (c) Schematic of the high dimensional dataset, where 3 configurations; 2 device placements; 14 frequencies; each with two impedance values (resistance, R and reactance, X) give a total of 168 ($3 \times 2 \times 14 \times 2$) values per participant. The data are reduced from 168 values to the single tensor EIM value in a two-step procedure: NTF (non-negative tensor factorisation), followed by PCA (Principal Component Analysis).

Table 2

Description of clinical signs of disease scoring. The overall score was calculated as a sum of all three clinical sign scores (0–7).

Clinical Sign	Description and corresponding score			
Tongue wasting	None: 0	Minimal: 1	Moderate: 2	Severe: 3
Tongue weakness	None: 0	Movement inside and outside mouth: 1	Movement only inside mouth: 2	Paresis: 3
Fasciculations	Absent: 0	Present: 1		

non-negative tensor factorisation was performed, where the high dimensional data were represented by contributions from dominant spectral shapes. For the interested reader, the mathematical outline is included in Supplementary Methods S2. This algorithm combines the contribution of each spectral shape into a single tensor EIM score, which was then used to monitor disease changes.

To first evaluate the group trend with time, a four-dimensional factorisation was employed (dimensions: 28 spectral features; 6 measurement types; each participant; 2 timepoints, baseline and 6 months). This was repeated for the ALS patient group and healthy volunteers and the average spectral pattern at each time point was calculated. Additionally, a comprehensive measure of individual participant’s spectral signature at each visit was calculated through a three-dimensional factorisation (dimensions: 28 spectral features; 6 measurement types; each participant measurement visit) followed by principal component analysis, to return the tensor EIM score. Absolute longitudinal change of the tensor EIM was

analysed with a linear-mixed model using a compound symmetry covariance matrix, fitted using Restricted Maximum Likelihood. Assessment of change was through the mixed model and using Mann-Whitney U tests in comparison to the healthy controls.

2.3. Sample size estimation

Estimating sample size requirements in hypothetical clinical trials have been utilised to assess the potential contribution of EIM to such studies (Rutkove et al., 2012; Shefner et al., 2018). The variation in the slopes of change of each metric was quantified using the effect size:

$$\text{Effect size} = \frac{\text{mean slope}}{\text{STD}} \tag{1}$$

For metrics with healthy control comparisons this is modified to:

$$\text{Effect size} = \frac{\text{mean slope}}{\text{STD} + \varepsilon} \tag{2}$$

where ε is the average slope of the healthy controls; this provides the statistical noise within the data and helps avoid an overestimate of the effect size. The sample size was estimated for a hypothetical clinical trial at 80% power and 5% significance level. This was calculated at 50% and 20% treatment effects.

3. Results

3.1. Exploring disease related tongue EIM changes at the level of the whole spectrum

On average the ALS patient group demonstrated a spectral shift to the right over time. By contrast, healthy participant spectra were stable (Fig. 2a). Of note, the shift in the ALS patient EIM spectra is in keeping with that associated with worsening disease severity (Schooling et al., 2021; Li et al., 2016; Li et al., 2012) (Appendix Figure A2).

However, when inspecting the raw spectra of individual patients, the change over time was often more complex. Some patients demonstrated consistent movement of the spectra to the right, while for others we observed transient shifts to the left, followed by spectral movement to the right (Fig. 2b). Out of the 28 patients, 13 had a consistent shift to the right, while 15 patients had spectra which demonstrated movement to the left on at least one occasion.

3.2. Longitudinal tensor EIM

In order to capture the effects of disease as completely as possible we utilised spectra from all recording locations and all electrode configurations via tensor EIM. The change in the tensor EIM metric ($\Delta T\text{-EIM}$) was then used to quantify the direction of spectral change. Histograms of the change from baseline for all patients are shown at 3 months ($n = 26$), 6 months ($n = 20$) and 9 months ($n = 14$) (Fig. 3a). These reveal that, to begin with, spectra shifted in equal proportions in both directions. As time progressed, more spectra shifted in the positive direction (Fig. 3b), which corresponds to the overall spectral shape shift to the right.

While the numerous spectra for each patient can be reduced to the single $\Delta T\text{-EIM}$ value, the algorithm can also extract the dominant spectral patterns within the data (Fig. 3c). When $\Delta T\text{-EIM}$ is positive, the contribution from the spectral shape shown in red increases, while that in blue decreases (resulting in an overall spectral shift to the right). By contrast, when $\Delta T\text{-EIM}$ is negative, the contribution from the spectral shape shown in blue increases, and that in red decreases (encompassing an overall spectral shift to the left). The tensor EIM patterns were subsequently parameterised through simple circuit modelling to offer insight into the potential cellular changes underpinning these spectral shapes (Supplemental Methods S3, Appendix Figure A1).

To assess the sensitivity of tensor EIM for monitoring disease progression, the absolute value of $\Delta T\text{-EIM}$ was used in order to resolve the bidirectional change in spectral shape. Longitudinal linear mixed modelling demonstrated a significant change of tensor EIM with time (Fig. 4a). The measures of tongue strength,

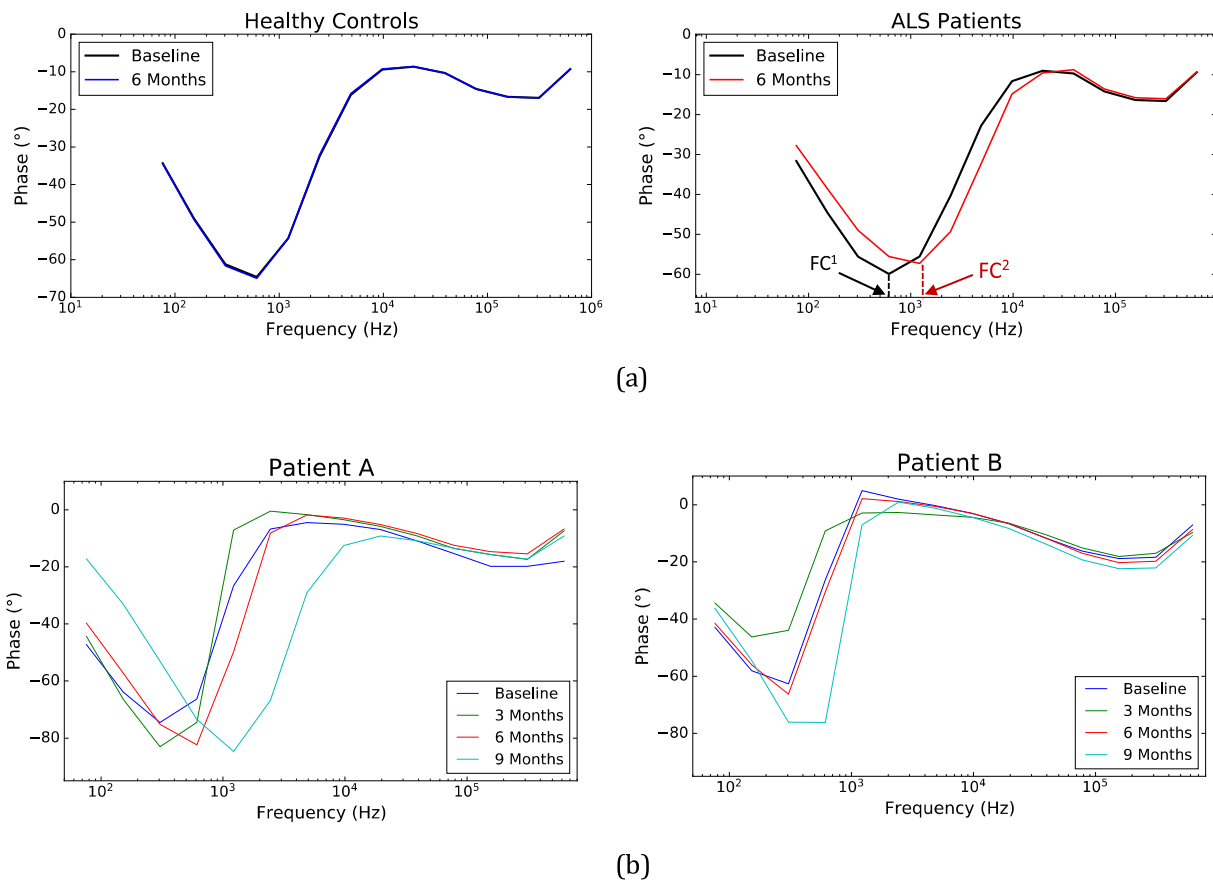
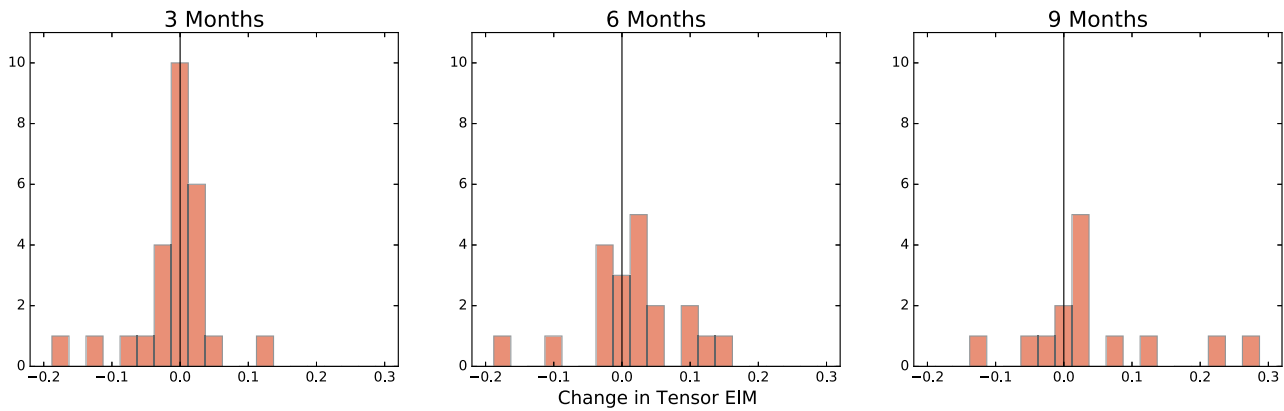


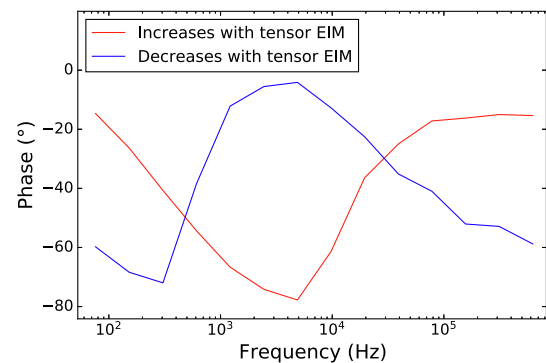
Fig. 2. (a) Group average in spectral change from baseline to six months for the healthy controls and ALS (Amyotrophic Lateral Sclerosis) patient group. The healthy group is stable in time. The ALS patient group trend is a shift right in the spectra, characterised by an increase in centre frequency (Fc) from Fc¹ to Fc². (b) Two examples of individual patient change. Patient A presents consistent shifts to the right with time, while patient B presents an initial shift left followed by progression to the right.



(a)

Month	3	6	9
Unchanged	10 (38%)	3 (15%)	2 (14%)
Negative shift	8 (31%)	6 (30%)	3 (21%)
Positive shift	8 (31%)	11 (55%)	9 (64%)

(b)



(c)

Fig. 3. (a) Individual patient Δ T-EIM (Change in tensor electrical impedance myography) from baseline at three time intervals. (b) A table summarising the number of patients whose spectra move in each direction or are unchanged after each time point. (c) A simple representation of tensor EIM as two contrasting spectral patterns. The positive shifts (or increases) in tensor EIM seen in (a) correspond to the spectral shape in red, which shows a shift to the right (increase in centre frequency). A negative shift (or decrease) in tensor EIM corresponds to the spectral shape moving left (blue; decrease in centre frequency).

ALSFRS-R bulbar subscore and the overall bulbar disease burden score demonstrated more limited change (Fig. 4b-d).

3.3. Clinical trial design

To illustrate the potential of tensor EIM for the detection of bulbar disease, a hypothetical clinical trial sample size was calculated (Table 3). Tensor EIM required the smallest sample size in comparison to other measures of symptoms. Trial size required when using raw data with a single frequency, as typically employed in EIM studies on ALS (Rutkove et al., 2012; Shefner et al., 2018), has a large variation depending on the frequency and electrode configuration selected but the best performing single frequency did not surpass the performance of tensor EIM.

4. Discussion

Herein we have presented evidence that a new analysis framework called tensor EIM is able to capture ALS-related changes within the highly complex ultrastructure of the tongue muscle. Development of biomarkers for bulbar disease in ALS is an area of unmet need and these results indicate that high dimensional EIM data can be utilised to provide a disease sensitive characterisation.

Most EIM technology captures information at a range of frequencies but the majority of studies to date have only made use of one or two frequencies (Rutkove et al., 2012; Rutkove et al.,

2014; Shefner et al., 2018). The increasing use of multiple electrode configurations adds further information about the state of the underlying muscle but also increases the amount of data collected (Luo et al., 2021). This generates a large (or ‘high dimensional’) dataset. While a more complete tissue characterisation is intuitively preferable, large datasets carry with them difficulties, such as the so-called ‘curse of dimensionality’. With this, a large number of observations not only risks reducing the generalisation of the results to other patients (overfitting) but also makes finding important patterns in the data more difficult (Kisil et al., 2018). By finding dominant spectra in a large EIM dataset, the tensor approach shows promise as a tool to maximise the potential of EIM as a biomarker for ALS and related conditions.

When assessing longitudinal EIM data at the level of the whole spectrum, we observed a complex and varied pattern of changes. The overall spectral shift to the right (or increase in centre frequency) over time is consistent with the progressive changes reported in mouse models of ALS (Li et al., 2016; Li et al., 2012), as well as in tongue and limb recordings from human patients (Mcilduff et al., 2017; Pacheck et al., 2016; Jafarpoor et al., 2011). We also observed transient spectral shifts in the opposite direction, in keeping with earlier work in animal models demonstrating that acute denervation can transiently shift impedance spectra in this fashion (Westgaard, 1975).

We have demonstrated for the first time in human ALS patients that the direction of spectral shift is complex and varied but we can only speculate as to what underpins this. Acute denervation results

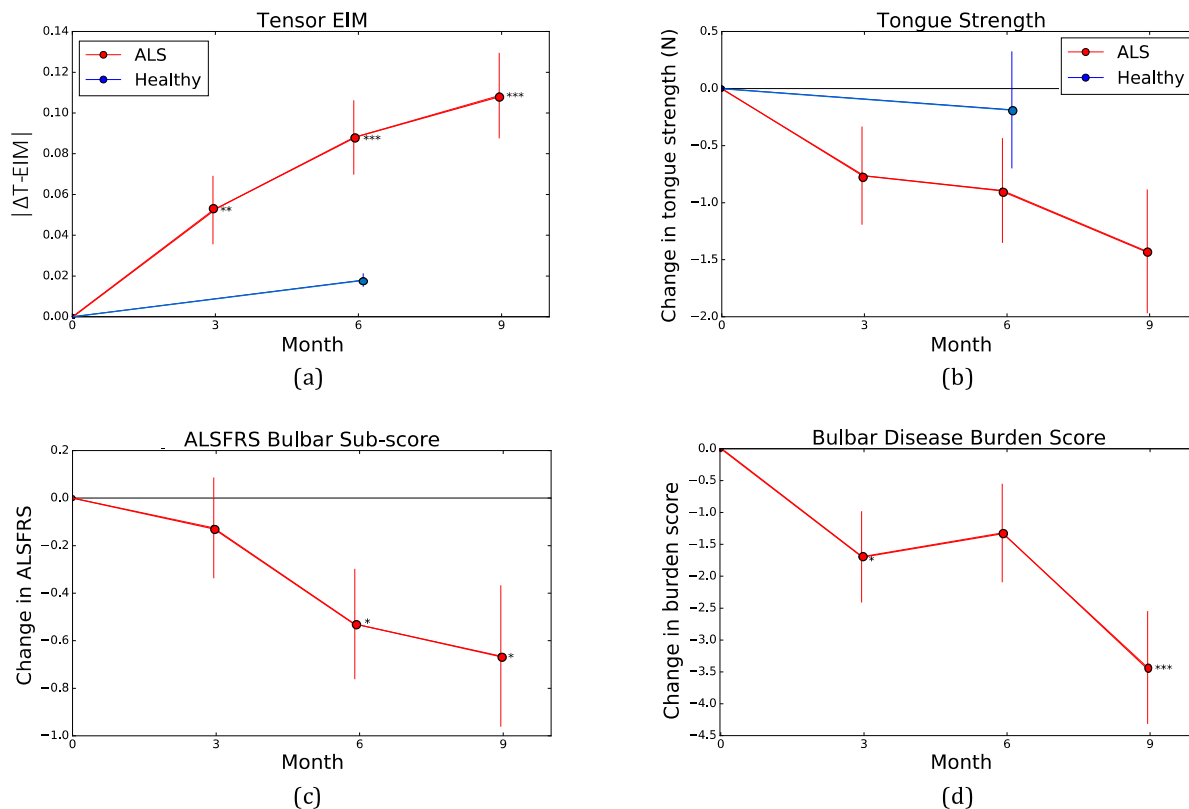


Fig. 4. Linear mixed models showing the change in biomarker values with time. (a) Absolute change over time of tensor electrical impedance myography ($|\Delta T\text{-EIM}|$) in patients and healthy controls. (b) Change in tongue strength over time in patients and healthy controls. (c) Change in patient ALSFRS-R (ALS Functional Rating Scale – Revised) bulbar sub-score. (d) Change in patient bulbar disease burden score. The error bars represent one standard deviation and significant p-values are marked as * $p < 0.05$, ** $p < 0.01$, *** $p < 0.001$.

Table 3

Effect size and hypothetical clinical trial sample size estimation with 80% power and 0.05 significance level at 50% and 20% treatment effects. Calculated for tensor EIM (Electrical Impedance Myography); the median and range values for single frequency raw EIM data; bulbar disease burden score; ALSFRS-R (ALS Functional Rating Scale-Revised); and tongue strength.

	Effect Size	Sample size at 50% treatment effect	Sample size at 20% treatment effect
Tensor EIM	0.99	64	401
Median single frequency	0.48	274	1715
Range single frequency	0.28–0.85	87–802	545–5014
Bulbar Disease Burden Score	0.84	89	558
ALSFRS-R Bulbar Sub-Score	0.46	298	1860
Tongue Strength	0.37	461	2881

in extracellular oedema (Kamath et al., 2008) (Carlson, 2014), which would act to reduce extracellular resistance and in turn shift spectral profiles to the left. Histological studies of muscle in ALS report myocyte hypertrophy (Jensen et al., 2016), which could, at least in theory, increase capacitance and also cause this spectral change. In contrast, authors of previous studies have attributed EIM changes in chronic settings to progressive myofibre atrophy (acting to reduce the overall tissue capacitance) and extracellular space remodelling (which would increase extracellular resistance). Our circuit modelling based on dominant spectral patterns found changes in extracellular resistance and membrane capacitance, which is in agreement with these suggestions (Appendix Fig-

ure A1). We thus tentatively hypothesise that the transient shift of spectra to the left relates to crescendos of denervation, while movement right represents the progression of chronic denervation-related changes. A preliminary stratification of EIM spectra by EMG findings potentially matches with these (Appendix Figure A3), but tongue EMG is fraught with technical difficulties. Further work relating EIM spectral patterns to EMG findings in other muscles may provide a better platform for testing our hypothesis.

An objective biomarker of bulbar disease would enhance ALS clinical trial design (Yunusova et al., 2019). The ability of tensor EIM to capture changes at the level of the whole EIM spectrum, across multiple electrode configurations and device placements likely underpins the reduced sample size requirements in the hypothetical clinical trial shown here. Previous studies on limb muscles utilising more limited spectral features have also shown EIM assessment of limb muscles can capture disease progression and reduce sample size, perhaps due to the sensitivity of EIM to the effects of both acute denervation and chronic denervation/reinnervation (Rutkove et al., 2020). In the present work, possibly owing to the complex muscle fibre arrangement in the tongue, we show that tensor EIM can provide further improvements, with a sample size around four times smaller than that of the average single frequency. Even an exhaustive search for the best performing frequency, which likely overfits the dataset (i.e., risks a type II error), does not perform as well as the tensor EIM method.

5. Conclusion

Tensor EIM appears to be capable of capturing the complex spectral fingerprint of ALS disease progression in the tongue. Spec-

tral change is described by a single tensor EIM metric, which can provide a simple measure for longitudinal studies. This approach enhances the potential of EIM as biomarker in ALS and could improve the monitoring of disease progression in clinical trials.

Declaration of Competing Interest

The authors declare that they have no known competing financial interests or personal relationships that could have appeared to influence the work reported in this paper.

Acknowledgements

The work was funded by Ryder Briggs Trust/Neurocare, United Kingdom (grant number RS8470), the Motor Neurone Disease Association, United Kingdom (grant number 918-793) and an Engineering and Physical Sciences Research Council Doctoral Scholarship (grant number EP/R513313/1). The work was also supported by the NIHR Sheffield Biomedical Research Centre (IS-BRC-1215-20017). PJS is supported as an NIHR Senior Investigator (NF-SI-0617-10077). The views expressed are those of the author(s) and not necessarily those of the NHS, the NIHR or the Department of Health. The authors wish to thank the participants for their time and generous contribution to research.

Appendix A. Supplementary material

Supplementary data to this article can be found online at <https://doi.org/10.1016/j.clinph.2022.04.015>.

References

Ahad MA, Narayanaswami P, Kasselmann LJ, Rutkove SB. The effect of subacute denervation on the electrical anisotropy of skeletal muscle: Implications for clinical diagnostic testing. *Clin Neurophysiol* 2010;121(6):882–6.

Alix JJP, McDonough HE, Sonbas B, French SJ, Rao DG, Kadiramanathan V, et al. Multi-dimensional electrical impedance myography of the tongue as a potential biomarker for amyotrophic lateral sclerosis. *Clin Neurophysiol* 2020;131(4):799–808.

Aram P, Shen L, Pugh JA, Vaidyanathan S, Kadiramanathan V. An efficient TOF-SIMS image analysis with spatial correlation and alternating non-negativity-constrained least squares. *Bioinformatics* 2015;31(5):753–60.

Bald EM, Nance CS, Schultz JL. Melatonin may slow disease progression in amyotrophic lateral sclerosis: findings from the pooled resource open-access ALS clinic trials database. *Muscle Nerve* 2021;63(4):572–6.

Calabrese EJ, Calabrese V, Giordano J. Demonstrated hormetic mechanisms putatively subserve riluzole-induced effects in neuroprotection against amyotrophic lateral sclerosis (ALS): Implications for research and clinical practice. *Ageing Res Rev* 2021;67:101273.

Carlson BM. The biology of long-term denervated skeletal muscle. *Eur J Transl Myol* 2014;24(1):5–11.

de Carvalho M, Dengler R, Eisen A, England JD, Kaji R, Kimura J, et al. Electrodiagnostic Criteria for Diagnosis of ALS. *Clin Neurophysiol* 2008;119(3):497–503.

Escudero J, Acar E, Fernadande A, Bro R. Multiscale entropy analysis of resting-state magnetoencephalogram with tensor factorisations in Alzheimer's disease. *Brain Res Bull* 2015;119:136–44.

Gaige TA, Benner T, Wang R, Wedeen VJ, Gilbert RJ. Three dimensional myoarchitecture of the human tongue determined in vivo by diffusion tensor imaging with tractography. *J Magn Reson Imaging* 2017;26(3):654–61.

Holder D. Brief introduction to bioimpedance. *Ser Med Phys Biomed Eng Electr Impedance Tomogr* 2004;411–22.

Jafarpoor M, Spieker AJ, Li J, Sung M, Darras BT, Rutkove SB. Assessing electrical impedance alterations in spinal muscular atrophy via the finite element method. *Annu Int Conf IEEE Eng Med Biol Soc* 2011;2011:1871–4.

Jensen L, Jørgensen LH, Bech RD, Frandsen U, Schröder HD, et al. Skeletal Muscle Remodelling as a Function of Disease Progression in Amyotrophic Lateral Sclerosis. *BioMed Res Int*. 2016;2016:5930621.

Kamath S, Venkatanarasimha N, Walsh MA, Hughes PM. MRI appearance of muscle denervation. *Skeletal Radiol* 2008;37(5):397–404.

Kapur K, Sanchez B, Pacheck A, Darras B, Rutkove SB, Selukar R. Functional Mixed-Effects Modeling of Longitudinal Duchenne Muscular Dystrophy Electrical Impedance Myography Data Using State-Space Approach. *IEEE Trans Bio-med Eng* 2019;66(6):1761–8.

Kisil I, Calvi GG, Chichoki A, Mandic DP. Common and Individual Feature Extraction Using Tensor Decompositions: a Remedy for the Curse of Dimensionality? In: 2018 IEEE International Conference on Acoustics, Speech and Signal Processing (ICASSP). p. 6299–303.

Li J, Pacheck A, Sanchez B, Rutkove SB. Single and Modeled Multifrequency Electrical Impedance Myography Parameters and Their Relationship to Force Production in the ALS SOD1G93A Mouse. *Amyotroph Lateral Scler Frontotemporal Degener* 2016;17(5–6):397–403.

Li J, Staats WL, Spieker A, Sung M, Rutkove SB, Borchelt DR. A Technique for Performing Electrical Impedance Myography in the Mouse Hind Limb: Data in Normal and ALS SOD1 G93A Animals. *PLoS One* 2012;7(9):e45004.

Luo X, Gutierrez Pulido HV, Rutkove SB, Sanchez B. In vivo muscle conduction study of the tongue using a multi-electrode tongue depressor. *Clin Neurophysiol* 2021;132(2):683–7.

McIluff CE, Yim SJ, Pacheck AK, Rutkove SB. Optimizing electrical impedance myography of the tongue in amyotrophic lateral sclerosis. *Muscle Nerve* 2017;55(4):539–43.

Pacheck A, Mijailovic A, Yim S, Li J, Green JR, McIluff CE, et al. Tongue Electrical Impedance in Amyotrophic Lateral Sclerosis Modeled Using the Finite Element Method. *Clin Neurophysiol* 2016;127(3):1886–90.

Rutkove SB, Caress JB, Cartwright MS, Burns TM, Warder J, David WS, et al. Electrical impedance myography as a biomarker to assess ALS progression. *Amyotroph Lateral Scler Frontotemporal Degener* 2012;13(5):439–45.

Rutkove SB, Caress JB, Cartwright MS, Burns TM, Warder J, David WS, et al. Electrical impedance myography correlates with standard measures of ALS severity. *Muscle Nerve* 2014;49(3):441–3.

Rutkove SB, Narayanaswami P, Berisha V, Liss J, Hahn S, Shelton K, et al. Improved ALS clinical trials through frequent at-home self-assessment: a proof of concept study. *Ann Clin Transl Neurol* 2020;7(7):1148–57.

Rutkove SB, Sanchez B. Electrical Impedance Methods in Neuromuscular Assessment: An Overview. *CSH Perspect Med* 2019;9(10):a034405.

Sanchez B, Martinsen OG, Freeborn TJ, Furse CM. Electrical impedance myography: A critical review and outlook. *Clin Neurophysiol* 2021;132(2):338–44.

Schooling CN, Jamie Healey T, McDonough HE, French SJ, McDermott CJ, Shaw PJ, et al. Modelling and analysis of electrical impedance myography of the lateral tongue. *Physiol Meas* 2020;41(12):125008.

Schooling CN, Jamie Healey T, McDonough HE, French SJ, McDermott CJ, Shaw PJ, et al. Tensor electrical impedance myography identifies clinically relevant features in amyotrophic lateral sclerosis. *Physiol Meas* 2021;42(10):105004.

Shefner JM, Rutkove SB, Caress JB, Benatar M, David WS, Cartwright MS, et al. Reducing sample size requirements for future ALS clinical trials with a dedicated electrical impedance myography system. *Amyotroph Lateral Scler Frontotemporal Degener* 2018;19(7–8):555–61.

Shellikeri S, Yunusova Y, Green JR, Pattee GL, Berry JD, Rutkove SB, et al. Electrical Impedance Myography in the Evaluation of the Tongue Musculature in Amyotrophic Lateral Sclerosis. *Muscle Nerve* 2015;52(4):584–91.

Westgaard RH. Influence of activity on the passive electrical properties of denervated soleus muscle fibres in the rat. *J Physiol* 1975;251(3):683–97.

Xie P, Song Y. Multi-domain feature extraction from surface EMG signals using nonnegative tensor factorization. *IEEE Int C Bioinform* 2013:322–5.

Yunusova Y, Plowman EK, Green JR, Barnett C, Bede P. Clinical Measures of Bulbar Dysfunction in ALS. *Front Neurol* 2019;10:106.